Electrospray Modeling of Highly Viscous and Non-Newtonian Liquids

H. Moghadam, M. Samimi, A. Samimi, M. Khorram

Department of Chemical Engineering, Faculty of Engineering, University of Sistan and Baluchestan, P. O. Box 98164-161, Zahedan, Iran

Received 16 April 2009; accepted 12 February 2010
DOI 10.1002/app.32302
Published online 3 June 2010 in Wiley InterScience (www.interscience.wiley.com).

ABSTRACT: The electrohydrodynamic spraying of highly viscous and non-Newtonian aqueous solutions of sodium alginate were experimentally modeled with high direct-current electric fields. A prototype electrospray setup comprising a nozzle connected to a high-voltage counter electrode connected to earth and a curing facility to solidify the droplets was used. The main aim was initially set to extend the knowledge of the electrospray to highly viscous liquids, where shear thinning was the main rheological feature of fluid flow through the nozzle of the spray system. To model the process, the effects on the size of beads of the electric field strength, nozzle diameter, flow rate, and the material properties of density, viscosity, surface tension, and electrical conductivity were characterized. The size distribution of the beads was obtained after the droplets were cured in a calcium chloride solution with an image analyzer system. The rheological study, carried out on different concentrations of alginate solution (i.e., 1–3 w/v %), showed a significant reduction in the viscosity as a function of the shear rate. Considering the shear-thinning behavior of the solutions, in the modeling we applied the viscosity at the operational shear rate in the nozzle. Four dimensionless groups were introduced to obtain the relationship between the dimensionless group representing diameter and the other groups in the dripping and jet modes with statistical analysis of the experimental data. The proposed equations correlated the size of beads within ±10% deviations as compared to the experimental results. © 2010 Wiley Periodicals, Inc. J Appl Polym Sci 118: 1288–1296, 2010

Key words: gelation; modeling; particle size distribution

INTRODUCTION

Electrohydrodynamic (EHD) spraying is a method of liquid atomization in which an electrical force is applied in the direction of gravitational force on the surface of a capillary. In electrospraying, one subjects the surface of the liquid capillary at the outlet of a nozzle to shear stress by maintaining the nozzle at a high electric potential.[1] This leads to elongation and, consequently, separation of the droplet from the nozzle's tip. Better control of size, by the setting of an appropriate electric field intensity and liquid flow rate, is the advantage of EHD spraying over conventional methods of liquid spraying. The electrospray, in some cases, reduces the size of droplets further than conventional mechanical atomizers, even to less than 10 μm.[2] The formation of droplets with the desired size is an important process in many engineering operations, such as ink-jet printing, spray drying and atomization, dispersion, emulsification, and functional particle production.[3]

The number of works classifying the mechanisms of EHD spraying is small (Hayati et al.,[4] Cloupeau and Prunet-Foch,[5] Grace and Marijnissen,[6] and Shiryaeva and Grigorev[7]). Furthermore, those also do not include all of the phenomena. This is especially the case for highly viscous and non-Newtonian liquids, where the classical mechanisms of cone-jet or laminar-jet breakup may not readily describe the process. The theory of the dispersion of liquids into small charged droplets under an electrostatic field was initially derived by Lord Rayleigh a century ago for inviscid liquids.[8] Using a linearized stability analysis, Rayleigh showed that a jet broke up when the developed wavelength was greater than the circumference of the jet. Weber[9] extended the theory of Rayleigh to viscid liquids. He showed that the optimum wavelength for the jet breakup depended directly on the viscosity and inversely on the density and surface tension of the liquid. When an axisymmetric disturbance of a frequency is imposed on a laminar jet, a liquid cylinder one wavelength long may form one droplet, where the optimum frequency of droplet formation may be correlated to the material properties of surface tension, density,

Correspondence to: A. Samimi (a.samimi@hamoon.usb.ac.ir).

and viscosity as well as the process variables of volumetric flow rate of the liquid in the nozzle and the nozzle diameter.[10] Speranza et al.[11] reported their investigations on the effect of pulsating direct-current (dc) frequency on the jet breakup of viscous (40–140 mPa s) and conductive liquids made from different concentrations of poly(vinyl alcohol). They showed that, within a range of dc frequencies imposed on a laminar jet, the frequency of produced monosized droplets were equivalent to the imposed electric frequency and any increase in the pulsating dc frequency led to a similar increase in the number of droplets per second. They showed that the range of drop formation was reduced with increasing viscosity of the liquids. Jaworek and Krupa[12] classified several modes of electrospraying depending on liquid characteristics such as density, viscosity, electrical conductivity, and surface tension as well as operational parameters such as applied voltage, nozzle diameter, and flow rate. Samimi and Ghadiri[13] and Moghadam et al.[14] extended the investigations to a range of viscosities that was much higher than that tested previously (1000–5000 mPa s), employing liquids such as sodium alginate, which showed non-Newtonian behavior. They investigated the effects of the electric field strength, nozzle diameter, flow rate, viscosity, surface tension, and electrical conductivity of sodium alginate liquid on the size and shape of the cured beads. Jayasinghe et al.[15] recently used a dc electrospray method on highly viscous liquids in coaxial needles to encapsulate biological living cells. They showed the spraying of highly concentrated suspensions of living organisms under stable cone-jetting conditions. However, their approach was focused on the application of the electrospray and not on the modeling of the phenomena.

The main objective of this study was to model the EHD spraying of highly viscous and non-Newtonian liquids (i.e., sodium alginate solutions) with a high dc electric field intensity. The study followed investigations carried out previously by this team[13,14] to model the process and to validate the experimental results.

EXPERIMENTAL

Sodium alginate from (Sigma-Aldrich, Munich, Germany) was used to prepare highly viscous alginate solutions at various concentrations 1–3 w/v %. Calcium chloride (Merck, Darmstadt, Germany) was obtained from Merck to make a 3 w/v % gelling solution. All experiments were carried out at room temperature, about 27°C.

The image of the experimental setup and the flow chart of the process are shown in Figure 1. The alginate droplet surface at the tip of nozzle was subjected to electrical shear stress along the gravitational force. The liquid capillary was, consequently, elongated downward; this led to the separation of the droplets from the nozzle. The sodium alginate droplets dripped into a container of calcium chloride and were cured by it; this produced alginate beads. The solution was gently stirred with a magnetic mixer. We adjusted the distance between the nozzle's tip and the container by increasing the vertical height of the pump/nozzle setup, as it could modify sphericity of the cured bead because of the greater relaxation time for the droplets before curing. This was especially the case for very highly viscous solutions.

Digital images of the beads, captured by a charge-coupled device camera installed on microscope, were analyzed with Motic Images Advanced software (Hong Kong, China) to characterize the shape and size distribution of the droplets in each experiment. A large number of beads were assessed for the size analysis to obtain the mean size with equivalent projected area diameters. The initial sodium alginate solutions were subjected to a characterization test to determine the viscosity at different shear rates, surface tensions, densities, and electrical conductivities. More details about the experimental setup and methods were given by Moghadam et al.[14]

The size of the droplets formed in electrospraying was affected by two series of parameters; solution characteristics and process variables. The surface tension, electrical conductivity, viscosity, and density were the most important properties of the alginate solution, whereas the applied electric field intensity, flow rate, and nozzle diameter were the influencing process parameters. In this study, the opening diameter of the earthed counter electrode and the vertical distance between the nozzle and the earthed electrode were kept constant at 30 mm and 10 mm, respectively. Therefore, the applied voltage (Ø) was chosen as the process variable to change the intensity of the electric field (E_s), according to eq. (1):

$$E_s = \frac{4\oslash}{D_n \ln(\frac{8L}{D_n})} \quad (1)$$

where D_n is the nozzle diameter, and L is the distance between the nozzle and the counter electrode, respectively. As the solution properties, mentioned previously, were affected by the concentration change, the alginate concentration, along with the flow rate, nozzle diameter, and voltage, were set as the variable parameters.

Table I shows the setup values for the process variables in seven test groups. Each test group was carried out with eight voltages of 0, 2, 4, 5, 6, 7, 8, and 9 kV, with eight samples collected for the size analysis. The combination of three levels, three parameters of concentration, nozzle diameter, and flow rate

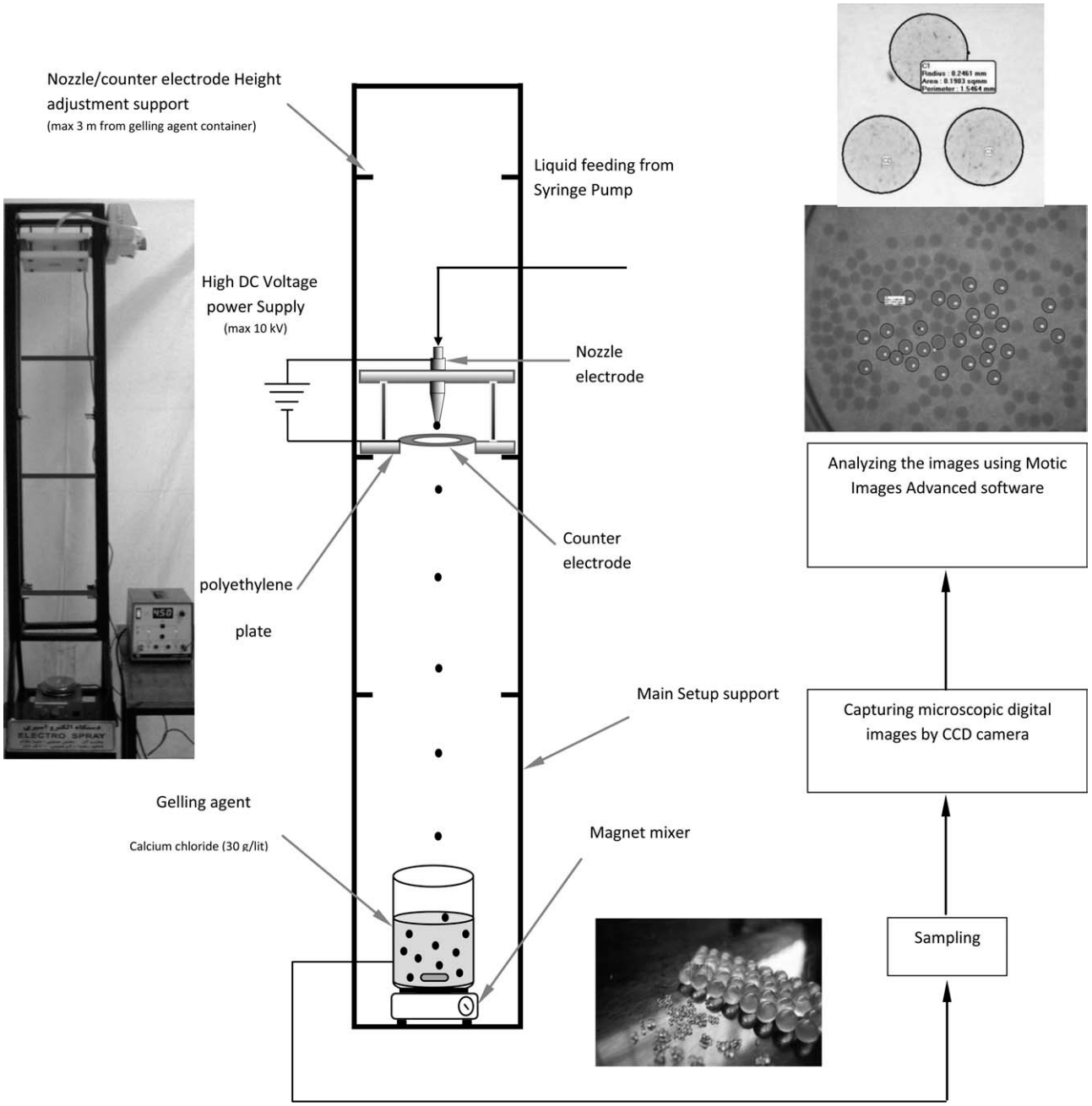

Figure 1 Image and flow chart of the experimental setup.

TABLE I
Operational Variables Considered in the Experiments

	Effect of C				Effect of D_n				Effect of Q			
Group no.	C (g/L)	D_n (mm)	Q (mL/h)	Group no.	C (g/L)	D_n (mm)	Q (mL/h)	Group no.	C (g/L)	D_n (mm)	Q (mL/h)
1	10	2	50	2	20	1	50	3	20	2	20
4	20	2	50	4	20	2	50	4	20	2	50
5	30	2	50	6	20	3	50	7	20	2	250

C = concentration.

TABLE II
Results of All of the Experiments at Different Levels and Operational Conditions

		Operational parameters				characteristics				Measured parameter
Group no.	Number of runs	Polymer concentration (g/L)	D_n (m)	Q (m^3/s)	Ø (V)	ρ (kg/m^3)	γ (N/m)	Viscosity (Pa s)	Electric conductivity (S/m)	Bead radius (mm)
1	1	10	0.002	1.39×10^8	0	1006	0.0732	0.123	1.96	1.8597
	2	10	0.002	1.39×10^8	2000	1006	0.0732	0.123	1.96	1.7601
	3	10	0.002	1.39×10^8	4000	1006	0.0732	0.123	1.96	1.5608
	4	10	0.002	1.39×10^8	5000	1006	0.0732	0.123	1.96	1.3374
	5	10	0.002	1.39×10^8	6000	1006	0.0732	0.123	1.96	1.0989
	6	10	0.002	1.39×10^8	7000	1006	0.0732	0.123	1.96	0.4902
	7	10	0.002	1.39×10^8	8000	1006	0.0732	0.123	1.96	0.3163
	8	10	0.002	1.39×10^8	9000	1006	0.0732	0.123	1.96	0.2945
2	9	20	0.001	1.39×10^8	0	1008	0.0757	1.09	3.88	1.6779
	10	20	0.001	1.39×10^8	2000	1008	0.0757	1.09	3.88	1.6133
	11	20	0.001	1.39×10^8	4000	1008	0.0757	1.09	3.88	1.3552
	12	20	0.001	1.39×10^8	5000	1008	0.0757	1.09	3.88	1.2039
	13	20	0.001	1.39×10^8	6000	1008	0.0757	1.09	3.88	0.9146
	14	20	0.001	1.39×10^8	7000	1008	0.0757	1.09	3.88	0.6191
	15	20	0.001	1.39×10^8	8000	1008	0.0757	1.09	3.88	0.4811
	16	20	0.001	1.39×10^8	9000	1008	0.0757	1.09	3.88	0.4854
3	17	20	0.002	5.56×10^9	0	1008	0.0757	1.09	3.88	1.84765
	18	20	0.002	5.56×10^9	2000	1008	0.0757	1.09	3.88	1.81555
	19	20	0.002	5.56×10^9	4000	1008	0.0757	1.09	3.88	1.5906
	20	20	0.002	5.56×10^9	5000	1008	0.0757	1.09	3.88	1.4944
	21	20	0.002	5.56×10^9	6000	1008	0.0757	1.09	3.88	1.1813
	22	20	0.002	5.56×10^9	7000	1008	0.0757	1.09	3.88	0.7811
	23	20	0.002	5.56×10^9	8000	1008	0.0757	1.09	3.88	0.4597
	24	20	0.002	5.56×10^9	9000	1008	0.0757	1.09	3.88	0.44611
4	25	20	0.002	1.39×10^8	0	1008	0.0757	1.09	3.88	2.0258
	26	20	0.002	1.39×10^8	2000	1008	0.0757	1.09	3.88	1.9926
	27	20	0.002	1.39×10^8	4000	1008	0.0757	1.09	3.88	1.7601
	28	20	0.002	1.39×10^8	5000	1008	0.0757	1.09	3.88	1.594
	29	20	0.002	1.39×10^8	6000	1008	0.0757	1.09	3.88	1.2667
	30	20	0.002	1.39×10^8	7000	1008	0.0757	1.09	3.88	0.9012
	31	20	0.002	1.39×10^8	8000	1008	0.0757	1.09	3.88	0.5321
	32	20	0.002	1.39×10^8	9000	1008	0.0757	1.09	3.88	0.5204
5	33	30	0.002	1.39×10^8	0	1012	0.0769	4.00	5.73	1.9581
	34	30	0.002	1.39×10^8	2000	1012	0.0769	4.00	5.73	1.9043
	35	30	0.002	1.39×10^8	4000	1012	0.0769	4.00	5.73	1.7179
	36	30	0.002	1.39×10^8	5000	1012	0.0769	4.00	5.73	1.5307
	37	30	0.002	1.39×10^8	6000	1012	0.0769	4.00	5.73	1.3018
	38	30	0.002	1.39×10^8	7000	1012	0.0769	4.00	5.73	1.1362
	39	30	0.002	1.39×10^8	8000	1012	0.0769	4.00	5.73	1.1192
	40	30	0.002	1.39×10^8	9000	1012	0.0769	4.00	5.73	1.2021
6	41	20	0.003	1.39×10^8	0	1008	0.0757	1.09	3.88	2.025
	42	20	0.003	1.39×10^8	2000	1008	0.0757	1.09	3.88	1.9764
	43	20	0.003	1.39×10^8	4000	1008	0.0757	1.09	3.88	1.7851
	44	20	0.003	1.39×10^8	5000	1008	0.0757	1.09	3.88	1.6576
	45	20	0.003	1.39×10^8	6000	1008	0.0757	1.09	3.88	1.49822
	46	20	0.003	1.39×10^8	7000	1008	0.0757	1.09	3.88	1.2751
	47	20	0.003	1.39×10^8	8000	1008	0.0757	1.09	3.88	0.7203
	48	20	0.003	1.39×10^8	9000	1008	0.0757	1.09	3.88	
7	49	20	0.002	6.94×10^8	0	1008	0.0757	1.09	3.88	1.9475
	50	20	0.002	6.94×10^8	2000	1008	0.0757	1.09	3.88	1.8271
	51	20	0.002	6.94×10^8	4000	1008	0.0757	1.09	3.88	1.7101
	52	20	0.002	6.94×10^8	5000	1008	0.0757	1.09	3.88	1.5243
	53	20	0.002	6.94×10^8	6000	1008	0.0757	1.09	3.88	1.2868
	54	20	0.002	6.94×10^8	7000	1008	0.0757	1.09	3.88	1.1303
	55	20	0.002	6.94×10^8	8000	1008	0.0757	1.09	3.88	1.0758
	56	20	0.002	6.94×10^8	9000	1008	0.0757	1.09	3.88	1.0257

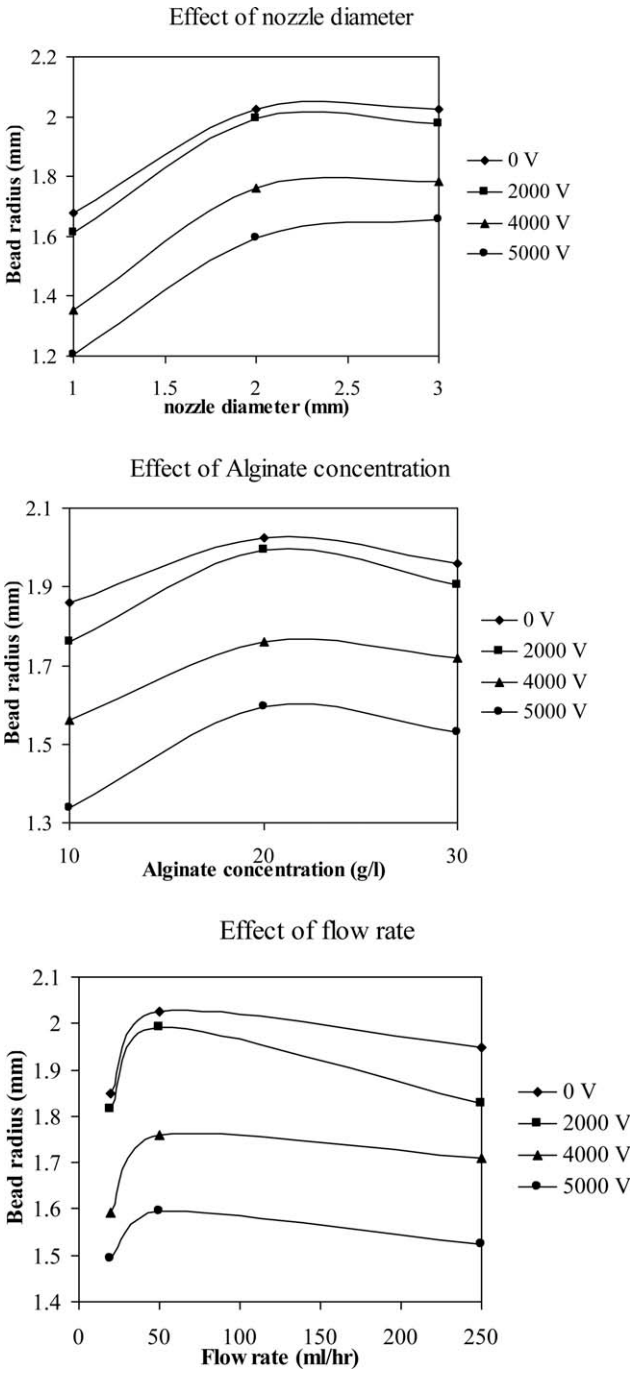

Figure 2 Effects of the nozzle diameter, alginate concentration, and liquid flow rate on the beads size at different voltages.

with eight voltages set up at least 56 experiments. Each experiment was repeated three times, and the measurements were averaged to obtain reliable results; therefore, about 170 beads samples in total were collected for the size analysis.

RESULTS AND DISCUSSION

All of the experiments were carried out according to Table I in seven different groups to investigate the effect of parameters mentioned previously on the size of beads. In each group, the parameters of concentration, nozzle diameter, and flow rate were set to be constant for different applied voltages. The results are presented in Table II.

TABLE III
Solution Characteristics at Different Alginate Concentrations

Sodium alginate concentration (g/L)	Solution characteristics			
	ρ (kg/m^3)	Electric conductivity (S/m)	γ (N/m)	Viscosity (mPa S)
10	1006	2.78	0.06043	1.23 × 102
20	1008	4.86	0.06238	1.09 × 103
30	1012	6.96	0.06948	4.00 × 103

Effects of the variable parameters on the size of the beads

The effects of the nozzle diameter, alginate concentration, and flow rate on the average size of beads are shown in Figure 2.

The effect of the nozzle diameter on the size of beads was obtained by comparison of the results of the group tests of 2, 4, and 6, as shown in Table II. Figure 2(a) represents the average size of the beads as a function of nozzle diameter at different voltages but at a constant alginate concentration of 20 g/L and a flow rate of 50 mL/h, respectively. As shown, increasing the nozzle diameter increased the average bead size. However, for the larger nozzles (2 and 3 mm), the diameter had no more effect.

In Table III, the solution characteristics are presented at different alginate concentrations in the range of setup experiments. We observed that, generally, the density, conductivity, surface tension,

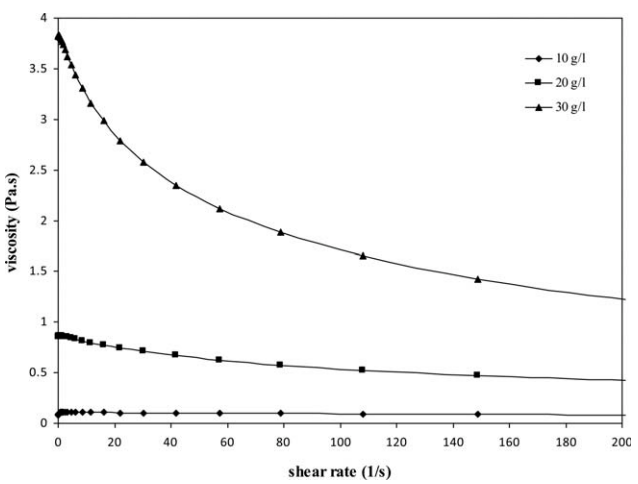

Figure 3 Rheological test results of different concentrations of sodium alginate solution.

TABLE IV
Viscosity of the Alginate Solution in the Limited Shear Rate Region of the Experiments

Group no.	D_n (m)	Flow rate (m^3/s)	Shear rate (1/s)	Viscosity (Pa s)		
				10 g/L	20 g/L	30 g/L
6	0.003	1.39×10^8	0.655	0.1068	0.861	3.8109
3	0.002	5.56×10^9	0.884	0.1078	0.861	3.7932
1, 4, 5	0.002	1.39×10^8	2.21	0.1087	0.8549	3.7044
7	0.002	6.94×10^8	11.052	0.1070	0.800	3.1907
2	0.001	1.39×10^8	17.684	0.1057	0.7643	2.9372

and viscosity (at zero shear rate) increased with concentration.

The effect of alginate concentration on size is shown in Figure 2(b) by a plot of the group test data of 1, 4, and 5 from Table II. The results initially represented an increase in average bead size with concentration from 10 to 20 g/L; then, it decreased slightly from 20 to 30 g/L. Increasing the concentration lead to an increase in the density, viscosity, surface tension, and electrical conductivity, as shown in Table III. However, a combination of the material properties affected by the concentration may have led to the trends shown in Figure 2(b) (i.e., the density and electrical conductivity had opposite relations with size, whereas the surface tension and viscosity behaved directly). This is discussed more in the modeling section.

The effect of the flow rate was investigated by a comparison of the group test data of 3, 4 and 7, as shown in Figure 2(c). The figure illustrates an initial increase in the bead size with flow rate (i.e., from 20 to 50 mL/h). However, it decreased when the flow rate increased five times from 50 to 250 mL/h. This was due to two different reasons. In low flow rates, the dripping mode of the spray may have dominated (20–50 mL/h), where an increase in the flow rate increased the droplets size. However, with further increases in the flow rate, a transition may have

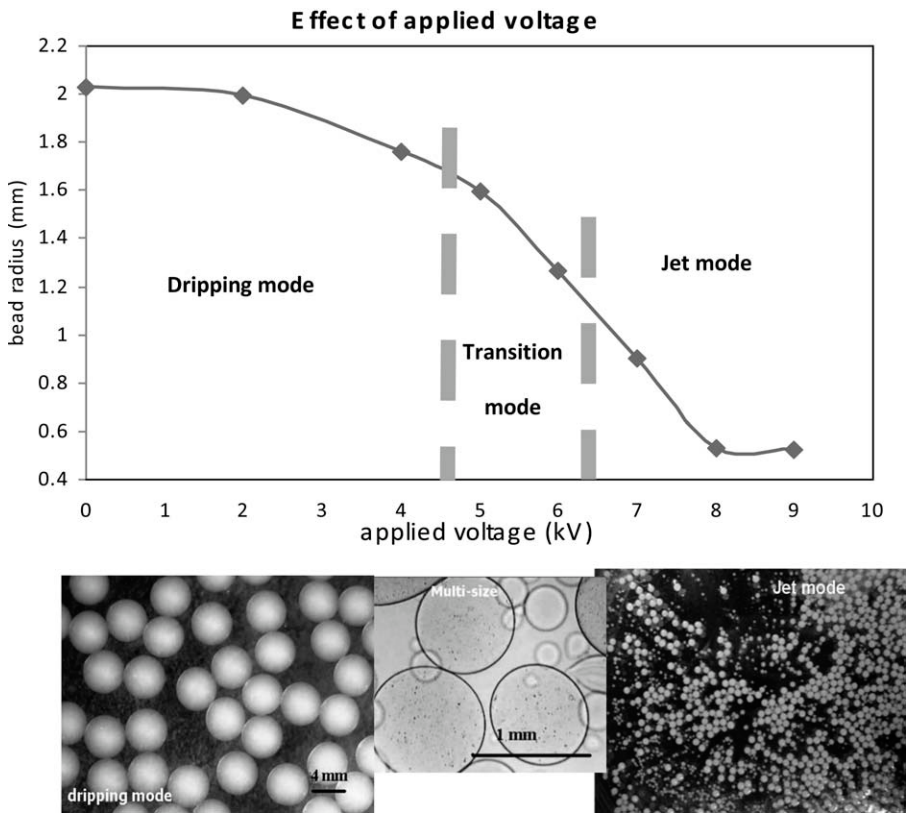

Figure 4 Effect of the applied voltage on the size of the beads and images of beads in three zones of dripping, transition, and jet modes.

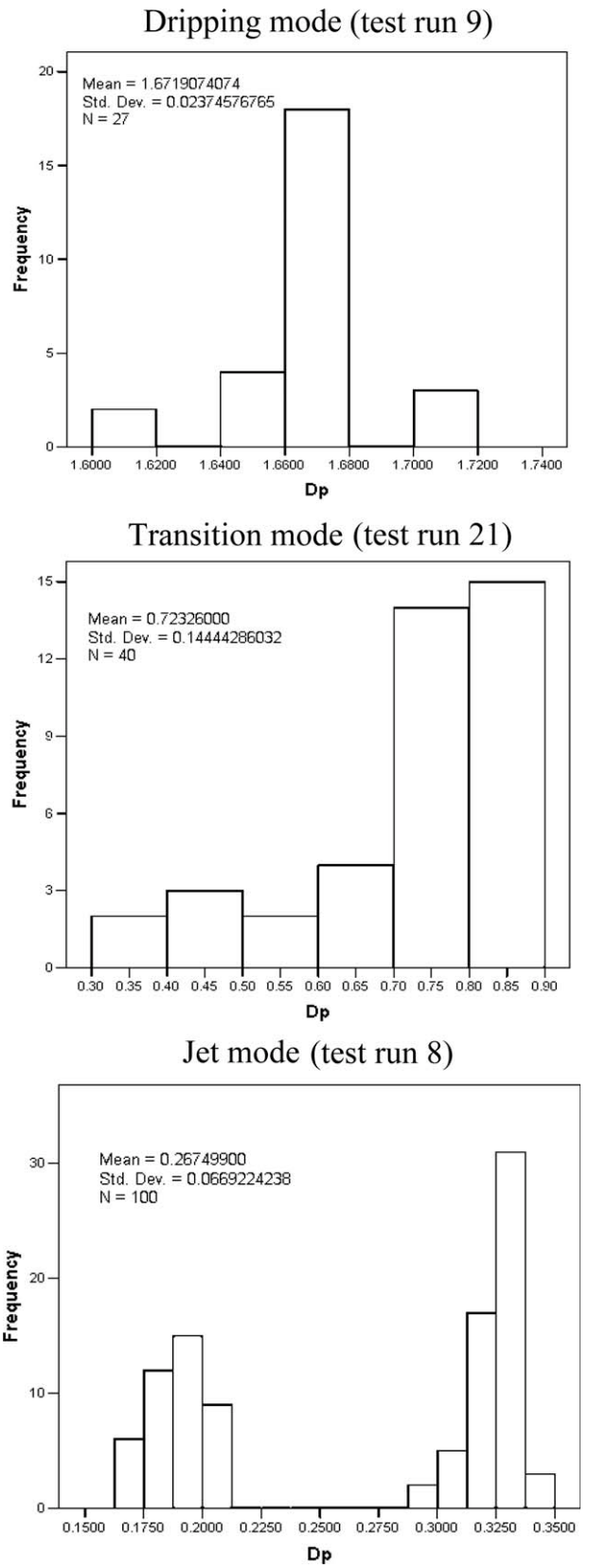

Figure 5 Differential size distribution of the beads in three regions of dripping, transition, and jet.

occurred from dripping to jet, by which the frequency of droplets increased while the size decreased (i.e., from 50 to 250 mL/h). Furthermore, the alginate solution showed non-Newtonian and shear-thinning behavior, where the viscosity decreased with increasing flow rate. Figure 3 illustrates the rheological behavior of the sodium alginate solution where its viscosity is plotted against the shear rate. As shown, for 20 and 30 g/L solutions, the shear-thinning characteristics were obvious, whereas the 10 g/L alginate solution looked to be Newtonian.

For non-Newtonian solutions, the viscosity depended on the shear rate at the tip of nozzle, where the flow rate (Q), nozzle diameter, and shear rate were related according to eq. (2):

$$\text{Shear rate} = \frac{4Q}{\pi D_n^3} \tag{2}$$

Table IV represents the viscosity of solutions at different concentrations in the limited range of shear rates applied in these experiments. The minimum shear rate (0.655 s^{-1}) corresponded to the lowest flow rate and highest nozzle diameter. In contrast, the maximum shear rate (17.684 s^{-1}) was related to the lowest nozzle diameter and the highest flow rate.

The effect of the applied voltage was investigated by a comparison of the bead size in each group of the experiments, where all of the parameters, except applied voltage, which was varied from 0 to 9 kV, were kept constant. This is shown in Figure 4, where an increase in the applied voltage had the most pronounced effect among all of the other parameters on the size reduction of the beads. As shown, in the early stages of voltage increase (i.e., up to about 5 kV), where the rate of size reduction was relatively low, the dripping mode dominated. However, within a range of voltage (ca. 4.5–6.5 kV), the size reduction sped up with voltage. In this range, a transition from the dripping mode to the jet mode occurred, whereas the frequency of droplet formation increased. In the narrow part of this range, where none of the spraying modes dominated, an unstable fluctuation between the dripping and the jet modes was observed; this caused a wide size distribution of beads. Over the transition voltage range (i.e., over about 8 kV), the size of beads stayed at a minimum value, where the jet mode of spraying dominated completely. Figure 5 represents the size analysis of the beads in the dripping, transition, and jet modes. With the mean size and standard deviation for each mode considered, the monosize distribution in the dripping mode (1.672 ± 0.024 mm), wide size distribution in the transition region (0.723 ± 0.144 mm), and bimodal size distribution in the

TABLE V
Experimental Parameter and Their Dimensions

Parameter	Dimension
D_b (bead diameter)	L
D_n	L
γ	MT^{-2}
μ	$ML^{-1}T^{-1}$
κ	$M^{-1}L^{-2}T^{3}A^{2}$
ρ	ML^{-3}
Q	$L^{3}T^{-1}$
E_s	$MLT^{-3}A^{-2}$

jet mode (0.268 ± 0.067) were the main size distribution features observed in these experiments.

MODELING OF THE ELECTROSPRAYING PROCESS

A good scaling law model of electrospraying should be able to predict the size of the beads under the operational conditions. In this regard, all the parameters that have an influence on the size of beads must be considered, and their effect should clearly be investigated. As mentioned earlier, there are complex effects of the flow rate and the solution concentration on the size of beads. The flow rate variation causes a change in the shear rate and, therefore, in the viscosity of non-Newtonian alginate solutions used in this study. On the other hand, it is well known that the surface tension and viscosity have a direct relation and the electrical conductivity and density have an inverse relation with the size of beads. Furthermore, the solution characteristics also depend on the concentration and should not be investigated individually. Dimensional analysis is a useful method dealing with the dimensions of the operational parameters and relates the size of the beads to the some dimensionless parameters. Table V represents all of the important parameters considered in this study and their dimensions.

Four dimensionless parameters were determined with eight affecting parameters and four basic dimensions (M, L, T, and A). With the density, nozzle outer diameter, surface tension, and electric field intensity considered repeating parameters, the four dimensionless groups were defined as follows:

$$D = \frac{D_p}{D_n} \tag{3}$$

$$R_e = \frac{\rho Q}{\mu D_n} \tag{4}$$

$$W_e = \frac{Q^2 \rho}{D_n^3 \gamma} \tag{5}$$

$$E = \frac{E_s^2 k D_n^4}{\gamma Q} \tag{6}$$

where D is the diameter number, R_e is the Reynolds number, ρ is the density, μ is the dynamic viscosity, W_e is the Webber number, γ is the surface tension, E is the electric field strength number, and κ is the electrical conductivity. These dimensionless numbers were determined with the known value of the parameters used in the experiments. With differences in the nature of droplet formation and its size in dripping and jet modes considered, the dependency of D on other dimensionless numbers was determined separately for these modes with SPSS software (http://www.spss.com). The following relationships

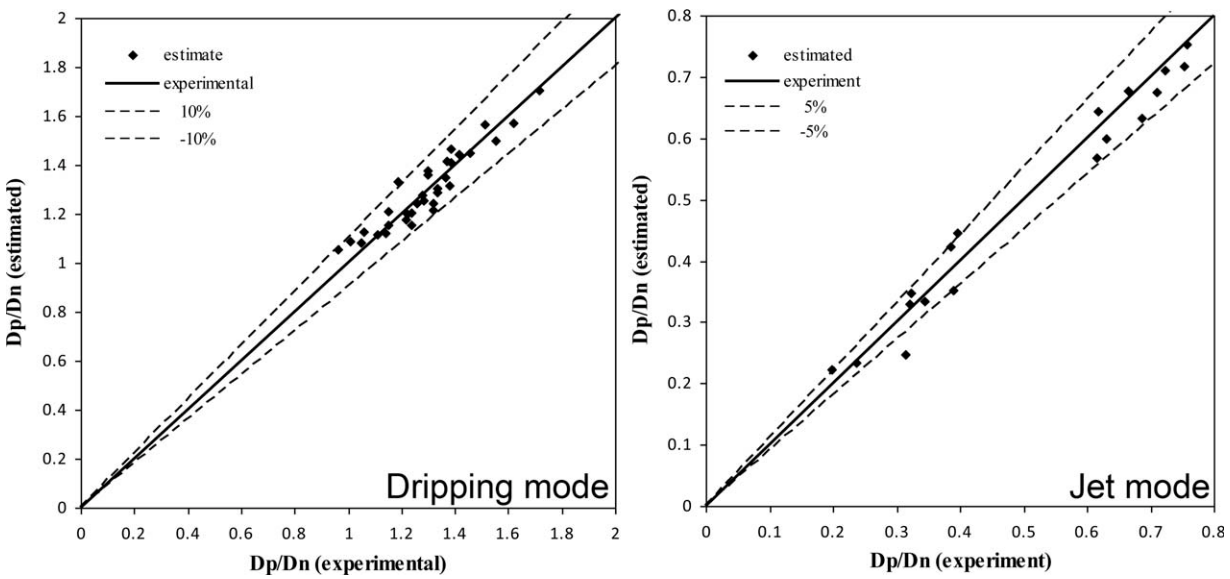

Figure 6 Comparison between the experimental and estimated dimensionless diameters: (a) dripping and (b) jet modes.

were obtained representing D as a function of the other dimensionless numbers in the dripping and jet modes, respectively:

$$D = 7.862(R_e^{-0.035} W_e^{0.046} E^{-0.059}) \quad (7)$$

$$D = (2.3114 \times 10^2)(R_e^{-0.37} W_e^{0.216} E^{-0.213}) \quad (8)$$

Figure 6 shows the comparison between the experimental and estimated values of dimensionless diameter in the dripping and jet modes. The dots in the figure are related to the modeling results. The figures show that both relationships estimated the size of beads within ±10% deviations from the experimental data.

CONCLUSIONS

This study extended the EHD-spray investigations to the higher range of liquid viscosity where the liquids behaved in a complicated manner. The sodium alginate used in this study showed non-Newtonian and shear-thinning behaviors in the concentration range 10–30 g/L. The effects on the size of cured calcium alginate beads of the material properties (electrical conductivity, density, viscosity, and surface tension) and the process variables (voltage, flow rate, and nozzle diameter) were investigated. With the non-Newtonian behavior of the alginate solution considered, the viscosity was determined at the operational shear rate at the nozzle tip. Two relations were suggested to predict the size of the beads in both the dripping and jet modes for such highly viscous solutions with dimensional analysis. Both relationships estimated the size of beads within ±10% deviations, as compared to the experimental results.

References

1. Jaworek, A.; Sobczyk, A. T. J Electrostatics 2008, 66, 197.
2. Watanabe, H.; Matsuyama, T.; Yamamoto, H. J Biochem Eng 2001, 8, 171.
3. Speranza, A.; Ghadiri, M. J Powder Technol 2003, 135–136, 361.
4. Hayati, I.; Bailey, A. I.; Tardos, T. F. J Colloid Interface 1987, 117, 205.
5. Cloupeau, M.; Prunet-Foch, B. J Electrostatics 1990, 25, 165.
6. Grace, J. M.; Marijnissen, J. C. M. J Aerosol Sci 1994, 25, 1005.
7. Shiryaeva, S. O.; Grigorev, A. I. J Electrostatics 1995, 34, 51.
8. Xie, J.; Lim, L. K.; Phua, Y.; Hua, J.; Wang, C. H. J Colloid Interface Sci 2006, 302, 103.
9. Weber, C. Angew Math Mech 1931, 2, 136.
10. Brandenberger, H.; Widmer, F. J Biotechnol 1998, 63, 73.
11. Speranza, A.; Ghadiri, M.; Newman, M.; Osseo, L. S.; Ferrari, G. J Electrostatics 2001, 51–52, 494.
12. Jaworek, A.; Krupa A. J Aerosol Sci 1999, 30, 873.
13. Samimi, A.; Ghadiri, M. Proceedings of Chemeca 2007, Icms Pty Ltd., Melbourne, Australia.
14. Moghadam, H.; Samimi, M.; Samimi, A.; Khorram, M. J Particuology 2008, 6, 271.
15. Jayansinghe, S. N.; Townsend-Nicholson, A. Lab Chip 2006, 1, 1018.